Wheaton Journal of
Neurobiology Research

Issue 9, Spring 2017:

"Modeling disease using primary neuronal tissue culture"

R.L. Morris, Editor. Wheaton College, Norton, Massachusetts.

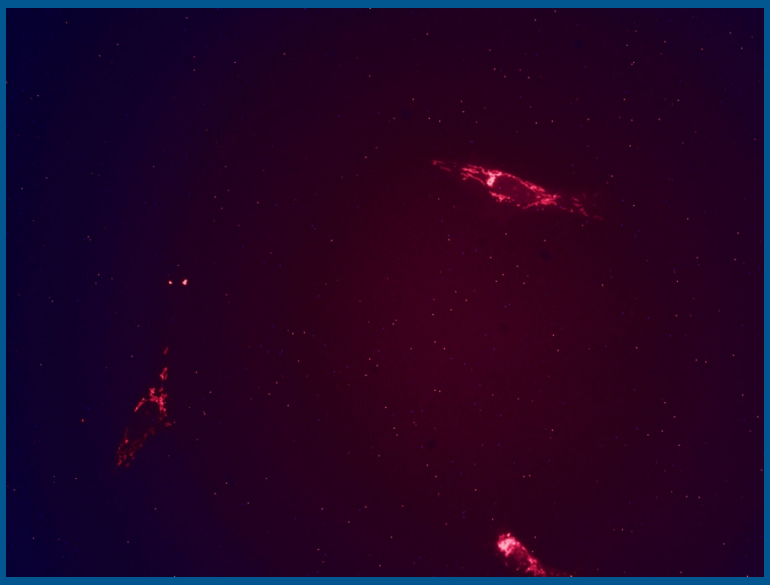

The effect of intracellular beta-amyloid on mitochondria activity as demonstrated through fluorescence microscopy

Claudine Humure

BIO 324 / Neurobiology
Final Research Paper
3 May 2017

The effect of intracellular beta-amyloid on mitochondria activity as demonstrated through fluorescence microscopy

Claudine Humure
Final Research Paper written for
Wheaton Journal of Neurobiology Research
BIO 324 / Neurobiology
Wheaton College, Norton Massachusetts
3 May 2017

Introduction

Alzheimer's Disease (AD) is a progressive neurodegenerative disorder that affects the brain's neurons or nerve cells and leads to memory loss, cognitive dysfunction and disturbs other intellectual abilities serious enough to interfere with daily life (Alzheimer's Association, 2017). Scientific research indicate that AD is linked to the presence of two main lesions that form in the brain: senile plaques composed of beta-amyloid (AB) protein, and neurofibrillary tangles made of intracellular *tau* proteins (Alzheimer, 2013). AB peptides are extracellular plaques that build up in spaces between nerve cells during the early onset forms of AD and are generated from the sequential cleavage of amyloid A4 protein precursor (APP), a plasma membrane protein (Murphy & Levine, 2010); Ashur-Fabian et al., 2003). To this day, it is not clear whether *Beta Amyloid* plaques cause AD or are the result of it (Ashur-Fabian et al., 2003).

Although AD is often associated with extracellular AB, studies suggest that intracellular AB appear as an early onset in the progression of AD, and that its levels decrease as extracellular plaques accumulate (LaFerla, Green, & Oddo, 2007). According to LaFerla et la, the first evidence to prove that AB may be generated intracellularly was recorded in 1993. Intracellular AB has been reported in brain parts that are likely to develop early AD pathology, such as the hippocampus and the entorhinal cortex (LaFerla et al., 2007). During AD, mitochondria suffer serious alterations that lead to the loss of calcium buffering capacity, reduced generation of adenosine triphosphate (ATP), and increased production of reactive oxygen species (ROS) (Moreira, Carvalho, Zhu, Smith, & Perry, 2010). All these alterations eventually lead to apoptosis as mitochondria fail to generate the energy needed for the normal functioning of the cells. Generally, mitochondria regulate energy metabolism and cell death pathways and are therefore responsible for providing the energy nerve cells need to carry out all their processes (Moreira et al., 2010). Neurons often concentrate mitochondria in areas with high ATP consumption, such as in synapses, active growth cones, etc. (Verburg & Hollenbeck, 2009).

In this study, the effect of intracellular *Beta Amyloid* on mitochondria activity found in glial cells was examined using chick embryonic peripheral neurons obtained from the embryos of domestic chicken, *Gallus gallus* (Clauer, 2017). Chick embryos are not only easy to obtain, but they are also able to grow large amounts of neurons at higher rates than other species such as rats (Matsuda, Baluk, Shimizu, & Fujiwara, 1996). A control group was set up where chick

sympathetic neurons were treated with Fluorescein Isothiocyanate-Dextran (FITC-Dextran) to track cell membrane permeability during trituration-loading of macromolecules into cells, and Rhodamine 123 (Rh 123), a fluorescent probe for staining mitochondria (Sigma, 1997; Johnson et al., 1980). The experimental group included intracellular AB loaded into cells by trituration-loading. We hypothesized that mitochondria activity in glial cells will decline due to the presence of intracellular AB fragment 25-35 as measured by fluorescent microscopy of Rhodamine 123. This experiment was conducted in collaboration with Christopher Lafen, Jake Newberry and Sophia black.

Materials and methods:

Primary Culture Dissection and ganglia dissociation

The dissection of chick embryos to harvest sympathetic nerve chains and dorsal root ganglion cells was performed following the protocol in the *Primary Culture of Chick Embryonic Peripheral Neurons1: Dissection* by Robert L. Morris adopted from a protocol by Peter J. Hollenbeck (Morris, 2015a). 1mg of beta-amyloid fragment 25-35 was purchased from Sigma Aldrich, category number A4559, to be used for the experimental condition in this study (Sigma, n.d.). We also bought Rhodamine 123 dye catalog number R302, for mitochondria labeling and FITC-Dextran dye, catalog number FD4, for tracking the beta amyloid movement from Sigma Aldrich.

Preparing the growth medium

A modified Leibovitz L-15 was converted to F-plus medium with neuronal growth factors and was used to grow neurons and glial cells. To prevent contamination, penicillin/streptomycin (pen/strep) was added to the growth medium (Morris, 2015a). Pen/strep protect against gram positive and negative aerobic and anaerobic bacteria but it does not protect against fungi or mold (Boundless, 2016).

Cell trituration

Following the trituration methods provided by Verburg & Hollenbeck (2009), the neurons and glial cells were triturated in order to open the membranes and permit FITC-Dextran and AB to enter the cell and go into the cytoplasm. For the control group, cells from one dish were triturated 20 times while other cells were triturated 60 times; for the experimental, all cells were triturated 20 times. For both the control and experimental groups, the isolated single cells were triturated with a volume of 25 mg/ml solution of FITC-Dextran similar to that of the cells and their growth medium combined. The experimental group was triturated with FITC-Dextran together with 3.42µl AB 25-35. The groups were incubated for 24 hours at 37^0C after being plated. The 3.42µl of AB was determined following the protocol from an article published in 2010 where the authors used 25µM solution of AB 25-35 at a dilution of 1:100 of the volume of cells and medium (Allaman et al., 2010). Based on this study we prepared our stock solution of AB to 25µM. This was the solution we used for trituration loading.

Cell washing and introducing Rh 123

Using the protocol by Sapiente (2017), all of the experimental petri dishes and one of the control dishes were washed with warm HBSS and treated with 2ml (2000µl) of Rh 123 after the 24 hour incubation. The Rh 123 was diluted at 1:11, 200 in HBSS. Two control dishes were exposed to Rh 123 while two others did not. The cells that were exposed to Rh 123 and the

control dishes were then incubated for 10 minutes at 37^0C before being washed again three times.

Making a chip chamber

Cell observations and chip were done as describe by Morris (2015b), with the following modifications. Microscope slides were placed on paper towel and a halo of chips on each of the slides was created using approximately 5-10 chips while making sure to avoid overlapping chips. A drop of empty growth medium from each of the dishes with cells par slide was obtained and placed in the middle of the halo using a Pasteur pipette. The coverslips were then lifted out of the growth medium with sharp forceps and carefully placed on top of the halo with the cell side facing downward. Cells were then located using transmitted light at a 10x magnification using phase 1 lens.

Fluorescent imaging

We used Nikon Eclipse E400 microscope to view the cells on the slides and take fluorescent images. On top of the microscope, Nikon Diagnostic Instruments 1.0x camera mount was positioned to enable the viewing and taking of images using Spot software. We first took both transmitted and fluorescent images at 40x magnification with phase 2 lens for the experimental group. To capture the images, we used Spot Insight Firewire 2 MegaPixel camera and the spot version 5.2.5 software that was already installed on the Apple Macintosh computer running OSX 10.10.5. The computers were in the ICUC lab at Wheaton College in Norton, MA. Several images were capture from all slides and three images from one of the slides were used for this experiment: transmitted image and two fluorescent images. One fluorescent image was staining for Rh 123 at an exposure time of 45,000-50,000 milliseconds in blue fluorescent light, and the other for FITC-Dextran at an exposure time of 9,000-10,000 milliseconds with green fluorescent light. We accounted for photo bleaching by avoiding multiple images in the same area. The same procedure was repeated to obtain the control group images: two transmitted images, two for FITC-Dextran solution and one for Rh123. All images were taken using a 40x objective lens and a phase 2 lens. All the above procedures were done in collaboration with my lab partners, Christopher Lafen, Jake Newberry, and Sophia Black.

Data Analysis

Two fluorescent images, one for the control and other for experimental, were uploaded into ImageJ that was downloaded from google on to a MacBookPro 13" (Figure 3 & 4C). Images were opened by holding command on the MacBookPro 13" keyboard, then selected and dragged into ImageJ (Minina, 2016). The analyze in the main toolbar was selected, *set measurements – area – min & max gray value – mean gray value* (this is what accounts for mitochondria activity) *–display label –ok*. The magnifying glass on the ImageJ toolbar was then selected, the image was zoomed into the cell of interest and the oval icon in the toolbar was selected to measure brightness (*analyze-measure).* A table accounting for every function that was selected appeared on the screen and the data for mean gray value were recorded into the excel sheet. The mean gray value of different bright spots on the cells appearing on the control images were selected. Threshold was set between 48 and 255, where any spot with a brightness lower than 48 was not considered to be a mitochondrion. Every spot with a brightness above 48 was studied. Setting threshold helped avoid bias while collecting the data. The same steps were repeated for the experimental image (Figure 4C). The data analysis was done using excel to generate a graph and calculate mean fluorescent intensity as well as the standard deviation for the data representing each group. A paired t-test was done to compare and analyze the data.

After collecting the necessary data to carry out statistical analysis, the control image with Rh 123 and all experimental images except for figure 4A were adjusted for brightness and contrast using Adobe Photoshop CC 2017. All images were adjusted to a contrast of 100. The Rh 123 control image was adjusted to a brightness of 150 (Figure 3). The experimental image with FITC (figure 4B) was adjusted to a brightness of 44 while the image in figure 4C with Rh 123 and AB 25-35 was adjusted to a brightness of 108. Image 4B was also adjusted to levels between 1.0 and 255.

Results:

Observations were made on three glial cells in the control group that went under 60 trituration loading strokes (Figure 1). The control images with FITC-Dextran solution (Figure 2) and Rh 123 (Figure 3) revealed brighter fluorescence in both channels than the experimental images that contained FITC-Dextran solution with AB 25-35 (Figure 4B) and Rh 123 with AB 25-35 (Figure 4C). This can be observed in the images depicting FITC-Dextran fluorescence, control (figure 2) and experimental (figure 4B). Figure 4B, also demonstrates that FITC-Dextran got caught up in the lysosomes as it cannot be digested by glial cells. We noticed that the cells triturated 20 times had dimmer cells than those that went through 60 trituration strokes (Figure 2). These data were collected in collaboration with Christopher Lafen, Jake Newberry, and Sophia Black.

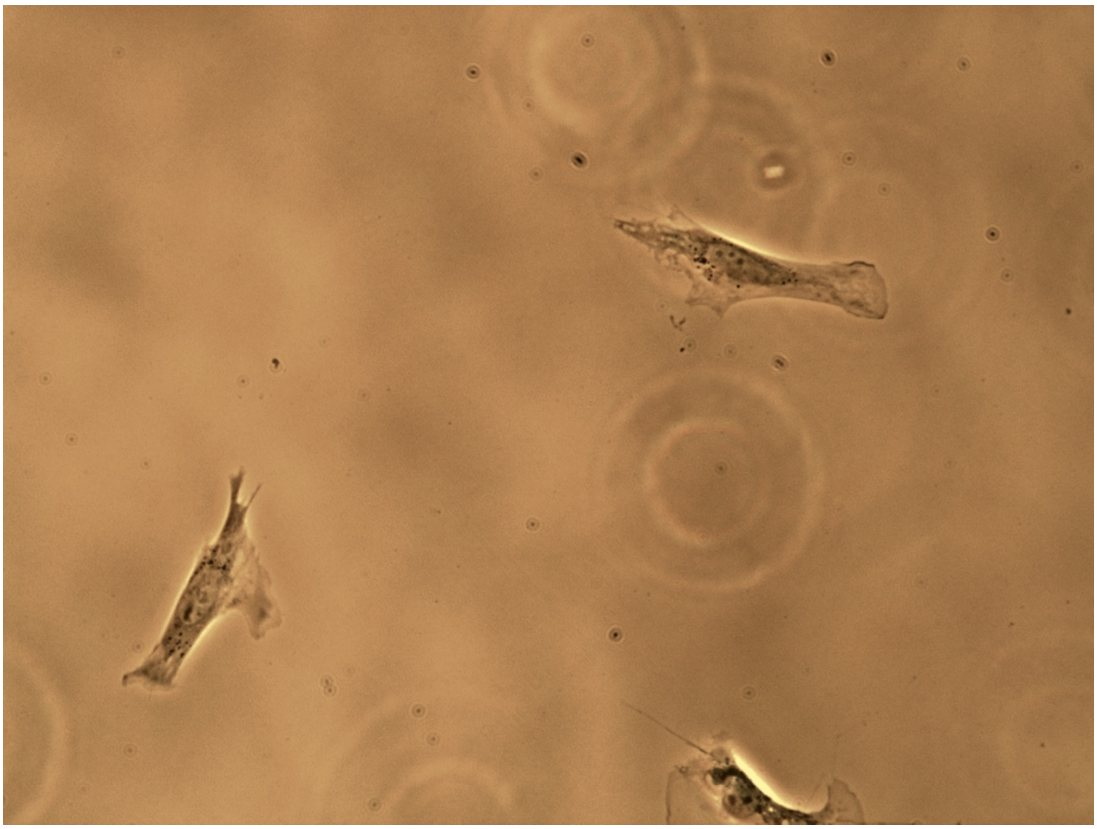

Figure 1: Transmitted image demonstrating 3 glial cells. Cells were treated with FITC-Dextran and Rhodamine 123 and were loaded with FITC-Dextran solution using 60 trituration strokes. Image was taken in collaboration with Christopher Lafen, Jake Newberry, and Sophia Black.

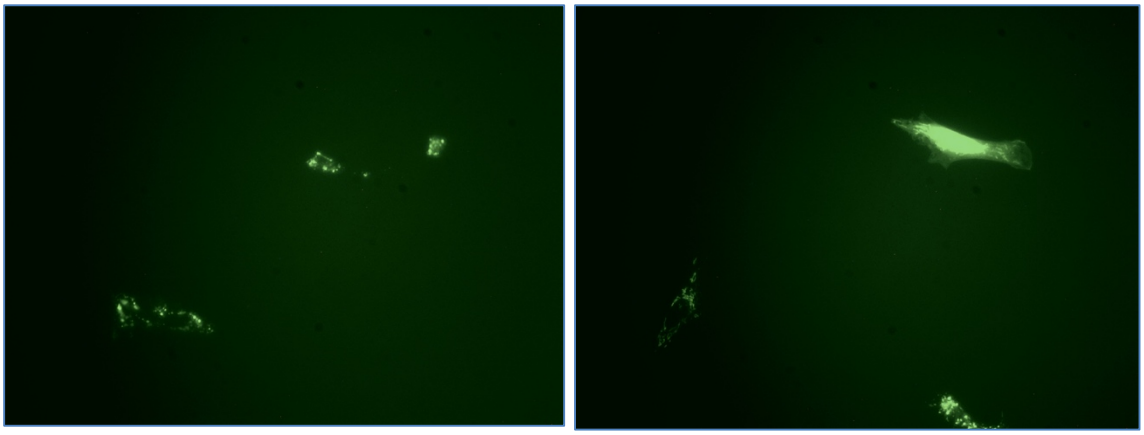

Figure 2: Fluorescent images stained with FITC-Dextran solution demonstrated by the green glow to indicate cell loading. These two images indicate that trituration loading worked. The cells in the image to the left went under 20 trituration strokes while the cells to the right are under 60 trituration strokes. This indicates that cells are more dose dependent when under increased trituration strokes than when fewer trituration strokes are applied. Images were taken in collaboration with Christopher Lafen, Jake Newberry, and Sophia Black.

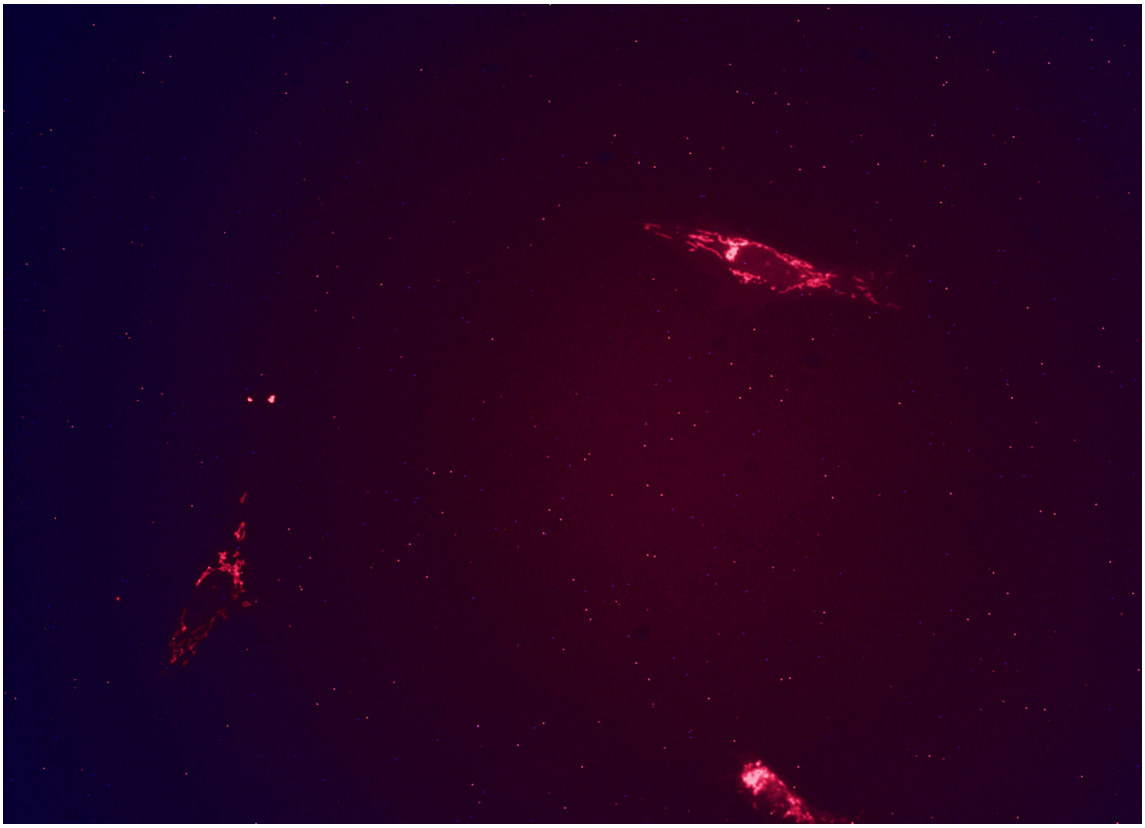

Figure 3: Fluorescent image of glial cells showing Rh 123 staining as demonstrated by the red glow to indicate mitochondria. These cells were triturated 60 times. The image was adjusted for brightness and contrast after data collection. Image was taken in collaboration with Christopher Lafen, Jake Newberry, and Sophia Black.

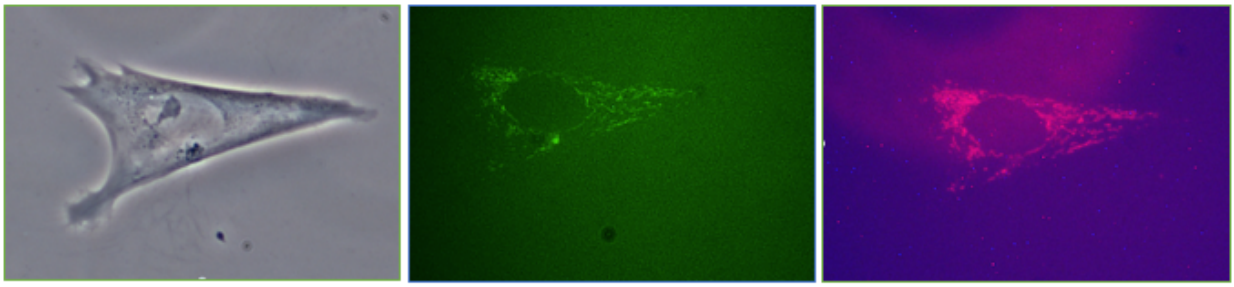

A B C

Figure 4: Experimental images with the same glial cell under different conditions. Transmitted image (A), Fluorescent image with a green glow to demonstrate that the cell was loaded with FITC-dextran and AB 25-35 (B). The background glow is due to an error made during cell washing. Image C is a fluorescent image with Rh 123 indicated by the red glow to demonstrate the presence of mitochondria. B and C were adjusted for brightness and contrast. This glial cell was triturated 20 times and loaded with 25mg/ml of AB25-35, stained with 2ml of Rh 123 and a 25mg/ml solution of FICT-Dextran. Images were taken in collaboration with Christopher Lafen, Jake Newberry and Sophia Black.

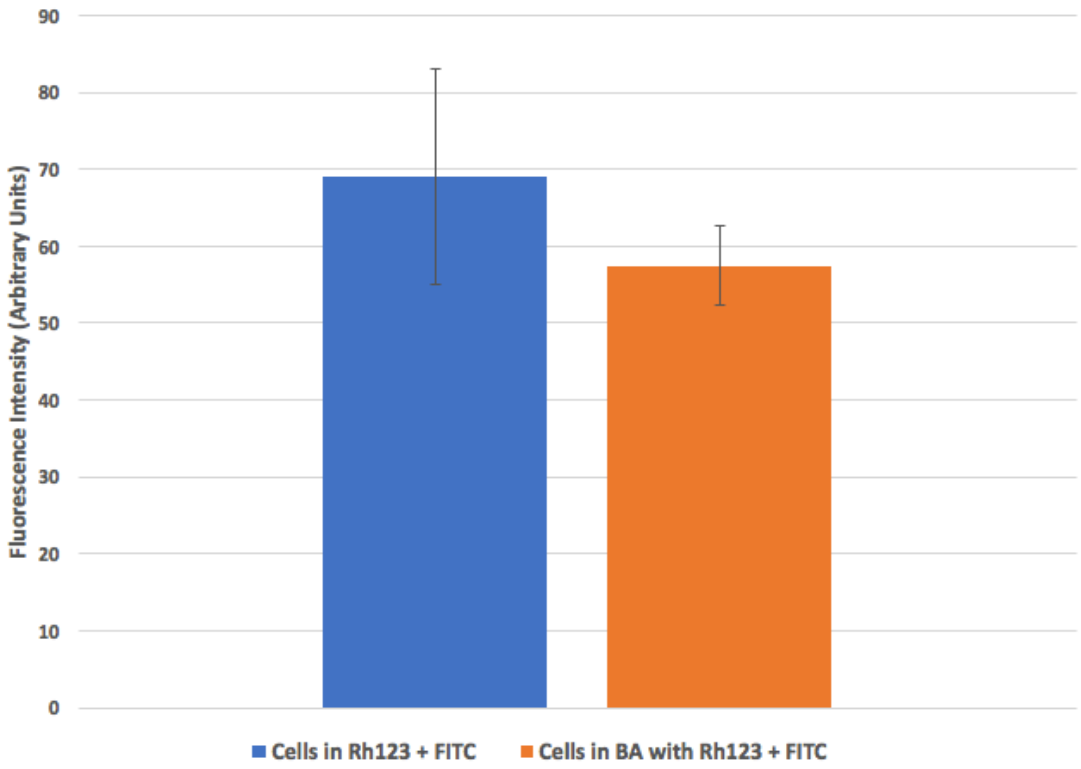

Figure 5: Average mean fluorescent intensity for the control (Rh123 +FITC-dextran) and the experimental (Rh123 + FITC-Dextran + BA) groups to indicate mitochondria activity. The sample size for the control group was n=3 glia, and for the experimental group n=3 glia. From each image we collected 21 samples of mean gray values from bright spots within a threshold of 48-255, where anything below 48 was not accounted for (Agnello, Morici, & Rinaldi, 2008).

Higher fluorescent intensity for the control group as compared to the experimental group was observed (Figure 5). A paired t-test was done to compare the data and using a two-tailed test, a p-value of 0.4 was obtained. Based on the p-value, I accepted the null hypothesis that there is no difference between the means and conclude that a significant difference does not exist. The standard deviation in figure 5 determined that most of the data collected for the group exposed to AB 25-35 are not significantly different from the control group.

Discussion & Conclusion:

While the data in the current study did not show a statistically significant difference in mitochondrial fluorescence between beta-amyloid-loaded cells and controls, the trend suggested that beta amyloid treatment may reduce mitochondrial activity (figure 5). Therefore, the hypothesis which states that lower mitochondria activity will be observed in glia that were exposed to intracellular AB as compared to the cells not exposed to AB cannot be accepted. The obtained p-value > 0.05, also confirms the conclusion that there is no significant difference between the experimental and the controls.

If this experiment gave the same results after being repeated a thousand times, then it would be concluded that these data are reliable. A large amount of data confirming that all the trends and differences between experimental and control are real would mean that the downward trend in the average fluorescent intensity (figure 5) did not only test the hypothesis, but it also demonstrates a significant difference in the mitochondrial fluorescence for both groups. From a cellular stand point, the trend would mean that the introduction of intracellular AB 25-35 caused the insoluble senile plaques to build up in the cytoplasm of the glia which disrupted internal processes and led to a decrease in mitochondria activity. In a study examining the effect of AB on permeability of inner mitochondrial membrane, it was concluded that AB has a direct influence on mitochondria where it affects the opening of specific mitochondrial channels and initiates programmed cell death (Shevtzova, Kireeva, & Bachurin, 2001). Like my experiment, the study from Shevtzova et al., (2001) indicates that AB negatively affects mitochondria. However, Shevtzova et al., (2001) specifically used mitochondria in rat liver which could be a source of significant difference when compared to my study, as the mitochondria of interest in both experiments are in different locations and came from different species. It is possible that some of our cells were contaminated during trituration loading. Also, cells were accidentally put back into the growth medium with FITC-Dextran solution during washing; an error that might have caused the loss of cells, hence n=1 (Figure 4B). In repeating this experiment, one could use a larger sample size and take precautions to prevent chances of error.

For future experiments, one could examine the molecular bonds between AB and mitochondria. There are a number of damages that AB plaques could cause when in contact with mitochondria and looking at the bonds between them would further clarify AB's effect on mitochondria function (Moreira et al., 2010). In a study examining the interaction between AB and mitochondria, it was mentioned that mitochondria function may be disturbed when AB blocks mitochondrial translocation of nuclear-encoded proteins (Pagani & Eckert, 2011). More studies need to be done regarding how AB affects cellular proteins and how it interacts with mitochondria membrane. Although many discoveries have been done about the nature of AD, the disease still has no cure and accounts for numerous deaths. Therefore, clinical and basic research must continue to be supported in hopes that we can one day find a cure for this prevalent disease.

Reference:

Agnello, M., Morici, G., & Rinaldi, A. M. (2008). A method for measuring mitochondrial mass and activity. *Cytotechnology*, *56*(3), 145–149. https://doi.org/10.1007/s10616-008-9143-2

Allaman, I., Gavillet, M., Belanger, M., Laroche, T., Viertl, D., Lashuel, H. A., & Magistretti, P. J. (2010). Amyloid-beta aggregates cause alterations of astrocytic metabolic phenotype: impact on neuronal viability. *J Neurosci*, *30*(9), 3326–3338. https://doi.org/10.1523/JNEUROSCI.5098-09.2010

Alzheimer's Association. (2017). Alzheimer's & Dementia Pathology | Alzheimer's Association. Retrieved February 16, 2017, from http://www.alz.org/alzheimers_disease_what_is_alzheimers.asp

Alzheimer, L. V. (2013). *Mechanisms and secrets of Alzheimer's disease: exploring the brain* (p. https://www.youtube.com/watch?v=dj3GGDuu15I). Retrieved from https://www.youtube.com/watch?v=dj3GGDuu15I

Ashur-Fabian, O., Segal-Ruder, Y., Skutelsky, E., Brenneman, D. E., Steingart, R. A., Giladi, E., & Gozes, I. (2003). The neuroprotective peptide NAP inhibits the aggregation of the beta-amyloid peptide. *Peptides*, *24*(9), 1413–1423. https://doi.org/10.1016/j.peptides.2003.08.005

Boundless. (2016). Types of Disinfectants. Boundless.

Clauer, P. (2017). History of the Chicken, 2017.

Johnson, L. V, Walsh, M. L., Chen, B., & Buchanan, J. M. (1980). Localization of mitochondria in living cells with rhodamine 123. *Froc. Natl. Acad. Sc. USA Cell Biology*, *77*(2), 990–994. Retrieved from http://www.pnas.org/content/77/2/990.full.pdf

LaFerla, F. M., Green, K. N., & Oddo, S. (2007). Intracellular amyloid-β in Alzheimer's disease. *Nature Reviews Neuroscience*, *8*(7), 499–509. https://doi.org/10.1038/nrn2168

Matsuda, S., Baluk, P., Shimizu, D., & Fujiwara, T. (1996). Dorsal root ganglion neuron development in chick and rat. *Anatomy and Embryology*, *193*(5), 475–80. https://doi.org/10.1007/BF00185878

Minina, A. (2016). Comparing intensities in different samples using ImageJ - YouTube. Retrieved April 18, 2017, from https://www.youtube.com/watch?v=E620JIg4CKw

Moreira, P. I., Carvalho, C., Zhu, X., Smith, M. A., & Perry, G. (2010). Mitochondrial dysfunction is a trigger of Alzheimer's disease pathophysiology. *Biochimica et Biophysica Acta (BBA) - Molecular Basis of Disease*, *1802*(1), 2–10. https://doi.org/10.1016/j.bbadis.2009.10.006

Morris, R. L. (2015a). Primary Culture of Chick Embryonic Peripheral Neurons 1: DISSECTION. Retrieved April 17, 2017, from http://icuc.wheatoncollege.edu/bio324/2015/NBlabPrimaryTissCultureProc1Dissn2015.htm

Morris, R.L. (2015b) Neurobiology Bio324 primary culture of chick embryonic peripheral neurons 2: observation of live unlabled cells. Accessed 11/04/2015. Available at: http://icuc.wheatoncollege.edu/bio324/2015/NBlabPrimaryTissCultureProc2ObservnOfLliveUnlabeledCells2015.htm

Murphy, M. P., & Levine, H. (2010). Alzheimer's disease and the amyloid-β peptide. *Journal of Alzheimer's Disease*. NIH Public Access. https://doi.org/10.3233/JAD-2010-1221

Pagani, L., & Eckert, A. (2011). Amyloid-Beta interaction with mitochondria. *International Journal of Alzheimer's Disease*, *2011*, 925050. https://doi.org/10.4061/2011/925050

Shevtzova, E. F., Kireeva, E. G., & Bachurin, S. O. (2001). Effect of β β β β β-Amyloid Peptide

Sapiente, J. (2017). Collaborator when determining rhodamine 123 concentration and how to use the reagent.

Fragment 25-35 on Nonselective Permeability of Mitochondria. *Byulleten□ Eksperimental□noi Biologii I Meditsiny*, *132*(12), 652–656. Retrieved from http://download.springer.com/static/pdf/803/art%253A10.1023%252FA%253A1014559331402.pdf?originUrl=http%3A%2F%2Flink.springer.com%2Farticle%2F10.1023%2FA%3A1014559331402&token2=exp=1492511108~acl=%2Fstatic%2Fpdf%2F803%2Fart%25253A10.1023%25252FA%25253A1014559331402.pdf%3ForiginUrl%3Dhttp%253A%252F%252Flink.springer.com%252Farticle%252F10.1023%252FA%253A1014559331402*~hmac=f90a1df91ed0b4527d295575ee691d523c6e88ef40b1e94d25c05f026c274fcc

Sigma. (n.d.). Amyloid β-Protein Fragment 25-35 ≥97% (HPLC) | Sigma-Aldrich. Retrieved April 30, 2017, from http://www.sigmaaldrich.com/catalog/product/sigma/a4559?lang=en&region=US

Verburg, J., & Hollenbeck, P. J. (2009). Mitochondrial Membrane Potential in Axons Increases with Local NGF or Semaphorin Signaling. *J Neurosci*, *28*(33), 8306–8315. https://doi.org/10.1523/JNEUROSCI.2614-08.2008.Mitochondrial

This experiment was done in collaboration with Christopher Lafen, Jake Newberry and Sophia Black.